Available online at www.sciencedirect.com
SCIENCE DIRECT
Trans. Nonferrous Met. Soc. China 16(2006) 766−771
Transactions of Nonferrous Metals Society of China
www.csu.edu.cn/ysxb/

Effects of Ag addition on mechanical properties and microstructures of Al-8Cu-0.5Mg alloy

SONG Min(宋 旼), CHEN Kang-hua(陈康华), HUANG Lan-ping(黄兰萍)

State Key Laboratory of Powder Metallurgy, Central South University, Changsha 410083, China

Received 30 September 2005; accepted 8 March 2006

Abstract: The mechanical properties and microstructures of Al-8Cu-0.5Mg alloy with and without Ag addition were studied at both room- and elevated-temperatures. The results show that the alloy with Ag is strengthened by a homogeneous distribution of coexistent θ' and Ω precipitates on the matrix (001) and (111) planes, respectively, whereas the alloy without Ag by θ' precipitates only. The small size and high volume fraction of θ' and Ω precipitates in the Ag-containing alloy improve the tensile strength and yield strength, especially those at the elevated temperatures. However, it is also responsible for the decrease in elongation, compared with the alloy without Ag, which is due to the microcracks initiated from the inherent incompatibility between the particles and the Al matrix during deformation.

Key words: Al-Cu-Mg alloy; mechanical properties; microstructures; Ag addition

1 Introduction

Heat-treatment aluminum alloys are required for many structural applications. And great efforts have been made to either improve the mechanical properties of the alloys currently being used or develop a completely new alloy series. The approaches adopted are either alloying modification, or processing modification, or both. The strength of aging-hardenable alloys such as Al-Cu-Mg series relies upon strengthening precipitates that form during aging after quenching. The aging schedules for such alloys are designed such that a uniform and fine distribution of precipitates results throughout the microstructure[1−3].

Small additions of some alloying elements are of prime importance to improve the mechanical properties. Such microalloying method has been widely applied to various alloy systems. In the Al-Cu-Mg alloy with high mass ratio of Cu to Mg, for example, the addition of Ag can improve the strength at both room- and elevated-temperatures[4]. This phenomenon is due to the formation of hexagon-shaped precipitate, designated Ω, on the matrix {111} planes[5,6]. Some previous studies [7, 8] show that the Ω phase has a face-centered orthorhombic structure (a=0.496 nm, b=0.895 nm, c=0.848 nm). CHANG and HOWE[9] have redesignated this phase as θ (a=b=0.606 6 nm, c=0.487 4 nm) on the basis that it has the same composition as the equilibrium θ phase (Al_2Cu), and they suggested that the precipitates have a tetragonal structure[10]. Actually, the differences in lattice parameter between the θ and Ω structural models are extremely small, and prolonged aging at temperatures above 250 ℃ results in eventual replacement of the $\{111\}_\alpha$ Ω precipitates by the equilibrium θ phase in a variety of orientations and morphologies[11]. Since the Ω phase reveals a good thermal stability at temperatures up to 200 ℃[12], it is a preferred strengthening phase in aluminum alloys for elevated-temperature applications.

Some recent works[13−16] studied the effect of Cu content and rare element Ce on the mechanical properties of Al-Cu-Mg-(Ag) alloy. These studies focus on the heat-treatment process and the addition of Ce on the mechanical properties of the alloy at elevated temperatures. However, the studies of the effect of precipitates on the strengthening and fractural mechanisms, and the precipitates coarsening mechanism are incomplete.

In this study, the effect of trace amount Ag on the mechanical properties and microstructures of Al-Cu-Mg alloy with a high Cu content (8%, mass fraction) was

Foundation item: Project(2005CB623704) supported by the State Key Fundamental Research Project on Al, China
Corresponding author: SONG Min; Tel: +86-731-8836773; E-mail: msong@mail.csu.edu.cn

reported, with the focus on the formation and coarsening of the θ' and Ω phases, and the effect of the precipitates on the strength and fracture.

2 Experimental

Two alloys were used in this study, they had the same composition as Al-8Cu-0.5Mg-(Mn, Ti, Zr) except for that alloy 1 contained no Ag, but alloy 2 had 0.6% Ag (mass fraction) addition. These alloys were prepared in an induction furnace in an argon atmosphere. The as-cast materials were homogenized at 500 ℃ for 10 h, followed by air cooling to room temperature. Then they were hot extruded with a ratio of 18 at 450 ℃. The extruded bars were solution-treated for 1 h at 250 ℃, and then water quenched. The bars were stretched slightly (about 1%) before artificial aging at 185 ℃ for various periods of time (from 2 to 20 h).

Vickers hardness measurement was performed on all aged samples. Those showing the highest hardness were selected for tensile testing at room temperature to 300 ℃. Fracture surface was studied by scanning electron microscopy(SEM) and the second phase constitution and precipitation by transmission electron microscopy(TEM). The TEM specimens were prepared by twin jet electro-polishing in a 30% nitric acid-70% methanol solution at −35 ℃ and examined by a JEM-100CXII microscopy operating at 100 kV.

3 Results

3.1 Vickers hardness

Fig.1 shows the vickers hardness (Hv) curves of the present two alloys. Both alloys show similar trend of the variation in Hv with aging time. That is, it increases as the aging time increases and reaches the highest value at 13 h. It then starts to decrease, showing over-aged phenomenon. Additionally, alloy 2 shows a higher hardness than alloy 1 at all stages.

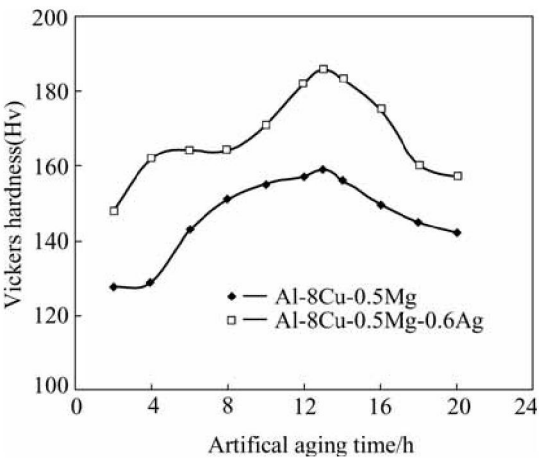

Fig.1 Vickers hardness of present alloys as function of artificial aging time

3.2 Tensile properties

The results of mechanical properties obtained from the two alloys at different temperatures are summarized in Table 1. Also the typical data for the 2618 alloy, which has a composition of Al-2.3Cu-1.6Mg-1.1Fe-1.0Ni-0.18Si-0.07Ti, are included for comparison.

Compared with alloy 1 without Ag, alloy 2 with Ag offers a considerable increase in tensile strength from 398 up to 478 MPa (above 20% improvement), whereas the yield strength from 279 to 433 MPa (about 55% improvement) at room temperature (20 ℃). Alloy 2 also shows increase in tensile strength (about 8%) and yield strength (about 23%) compared with the 2618 alloy at room temperature (20 ℃).

When compared with alloy 1 and 2618 alloy at elevated temperatures, alloy 2 shows simultaneous improvement in tensile strength and yield strength (Table 1) at different temperatures. And, the increase of strength is not at significant expense of the elongation as the tensile ductility decreases only slightly.

3.1 Fracture surface

Fig.2 shows the fracture surfaces of alloy 1 deformed at 20 ℃ and 300 ℃. Examination of these surfaces reveals some inter-granular cleavages surrounded predominantly by dimple rupture. Both the dimple diameter and the number of inter-granular cleavages are larger at 300 ℃ than those at 20 ℃.

Fig.3 shows the fracture surfaces of alloy 2 deformed at 20 ℃ and 300 ℃. The morphology of the fracture surfaces is similar to that of alloy 1, but the dimension of the dimples is much smaller than that in alloy 1.

3.4 TEM microstructures

The microstructure of the two alloys was investigated by TEM. The aim was to characterize the dependence of precipitation state on the alloy composition, and thus gain basic understanding of the relationship between mechanical properties and microstructures. The results are shown in Figs.4 and 5.

Figs.4(a) and (b) are for the precipitation of the θ' phase in alloy 1 at under-aged (4 h) and peak-aged (13 h) stages, respectively. It is found that this phase, which develops in {001} and {010} directions shows homogeneous distribution. Except for the θ' (Al_2Cu), Ω precipitates are hardly observed. Fig.4(c) shows the θ precipitates in the same alloy but at over-aged stage for 20 h. They have a spherical morphology with a size less than 40 nm, which is different from the planar morphology of the θ' phase seen in the alloy aged for 4 and 13 h. Fig.4(d) shows the selected diffraction pattern

Table 1 Mechanical properties of present and 2618 alloys at different temperatures

Specimen	Testing temperature/℃	Yield strength/MPa	Tensile strength/MPa	Elongation, δ/%
Alloy 1 (without Ag)	20	279	398	18.7
	150	310	354	16.6
	200	302	317	20.8
	250	265	281	29.9
	300	170	178	37.9
Alloy 2 (with Ag)	20	433	478	14.5
	150	418	426	13.9
	200	364	371	15.3
	250	301	306	15.3
	300	225	228	15.1
Alloy 2618	20	372	441	10
	150	303	345	14
	200	179	221	24
	250	62	90	50
	300	31	52	80

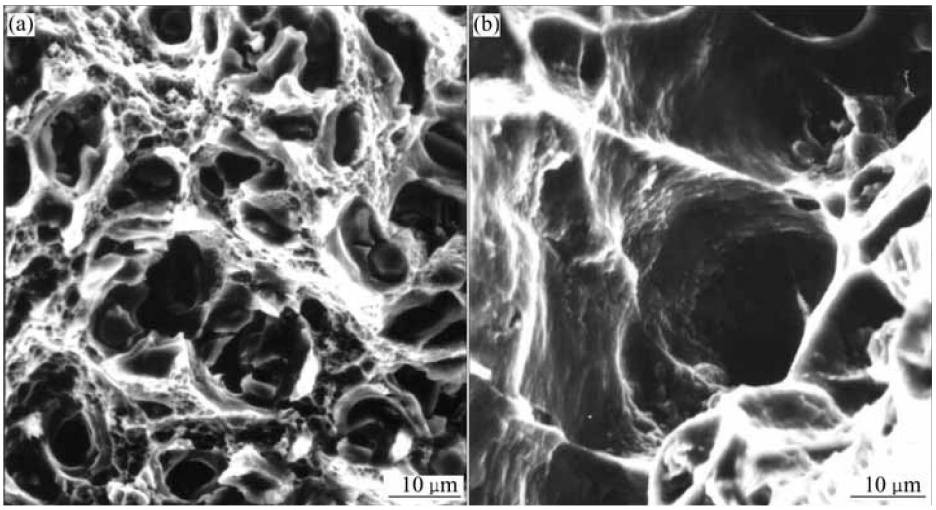

Fig.2 Fracture surface of alloy 1 at 20 ℃ (a) and 300 ℃ (b)

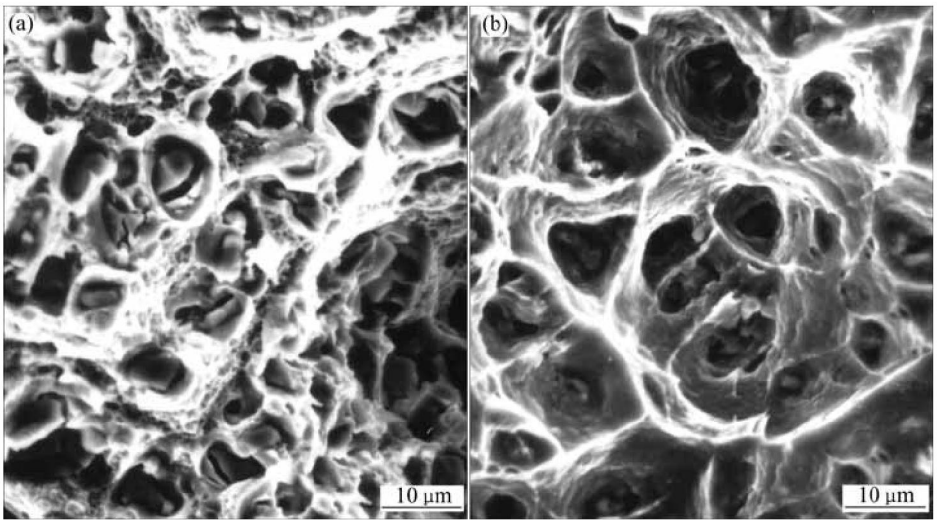

Fig.3 Fracture surface of alloy 2 at 20 ℃ (a) and 300 ℃ (b)

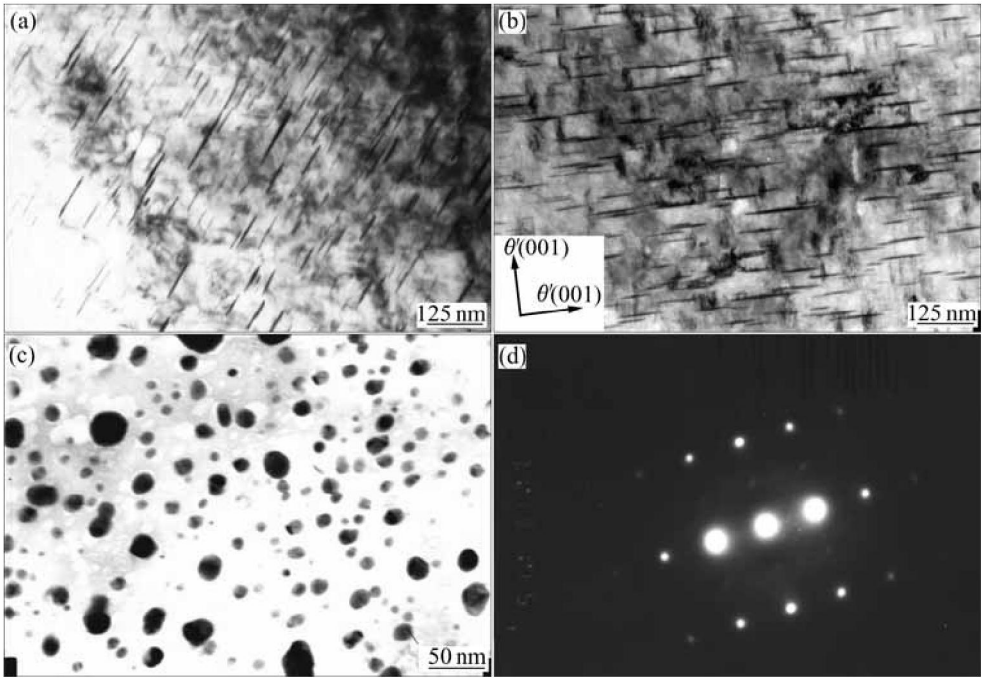

Fig.4 Precipitates in alloy without Ag: (a) θ' platelets at under-aged stage (4 h); (b) θ' platelets at peak-aged stage (13 h); (c) Spherical θ phase at over-aged stage (20 h); (d) Selected diffraction pattern of θ' phase

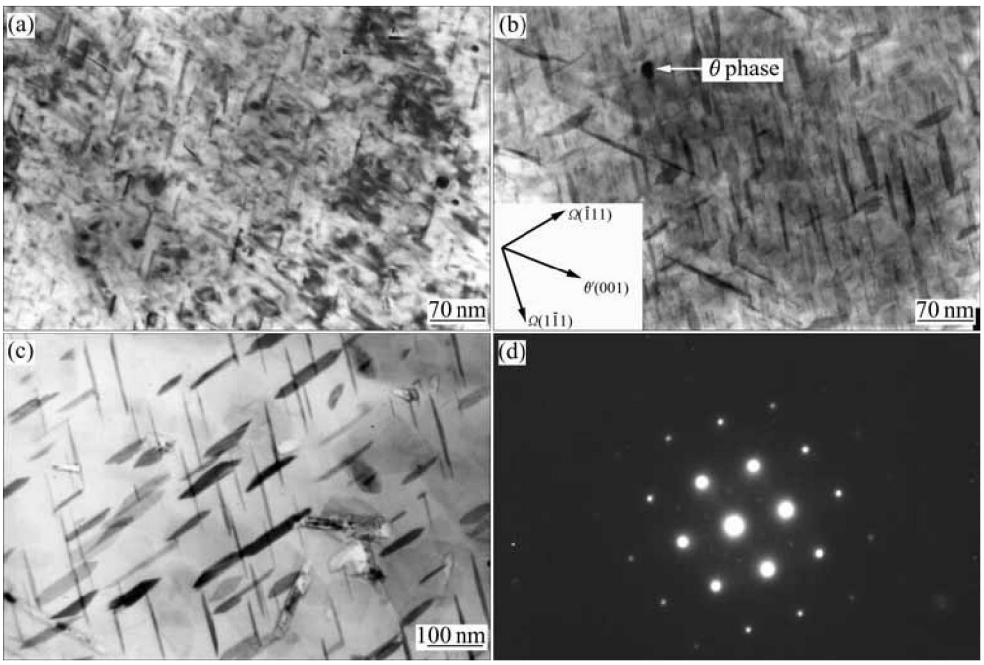

Fig.5 Precipitates in Ag-containing alloy: (a) Coexistence of θ' and Ω phases at under-aged stage (4 h); (b) Coexistence of θ' and Ω phases at peak-aged stage (13 h); (c) Ω phase at over-aged stage (20 h); (d) Selected diffraction pattern of Ω phase

of θ' phase.

Figs.5(a) and (b) illustrate the relationship of precipitates Ω and θ' (Al_2Cu) in alloy 2 at under-aged (4 h) and peak-aged (13 h) stages, respectively. It can be seen that the distribution of Ω and θ' is homogeneous and has a large volume fraction. The coexistence of Ω and θ' shows a special oriental relationship, where one θ' platelet develops in the {001} direction and two platelets develop in the $\{\bar{1}\,1\,1\}$ and $\{1\,\bar{1}\,1\}$ directions (Fig.5(a)), respectively. In addition to θ' and Ω phases, small amount of θ phase can also be found in some areas. Fig.5(c) shows the Ω precipitates in the same alloy but at over-aged stage for 20 h. It can be seen that Ω phase remains platelet shape even after aged for 20 h, which

increases the mechanical properties at elevated temperatures, compared to the alloy without Ag. Fig.5(d) shows the selected diffraction pattern of Ω phase.

4 Discussion

It has been shown that both the Vickers hardness and strength of alloy 2 are much higher than those of alloy 1. The main reason for the improvement is that the Ag addition induces a high density of coexistent precipitates of θ' and Ω with fine sizes in alloy 2. As shown in Fig.4(a), a lot of θ' precipitates which have a homogeneous distribution can be found but there is no Ω precipitate. The dimension of the θ' phase in alloy 1 is much larger and the volume fraction is much lower than those of θ' and Ω in alloy 2.

The large dimension and low volume fraction of the θ' phase in alloy 1 lead to a large spacing between precipitates. It is well known that the strength of Al alloys is mainly due to the particle/dislocation interaction. The dislocation must bypass or cut through the precipitates when they slip across the obstacles. Considering that θ' and Ω phases are platelet-like and very hard, which are difficult to be cut by dislocations, dislocations mainly bypass the phases by cross-slip. When dislocations slip across the precipitates, the yield stress τ can be calculated by the following equation[17]:

$$\tau = \tau_0 + a \cdot \mu \cdot b^{1/2} \cdot \gamma \cdot \lambda^{-1/2}$$

where τ_0 is the yield strength of the matrix without precipitates, μ is the shear modulus of the matrix phase, γ is the shear quantity, b is the Burgers vector of dislocations, λ is the spacing of the platelets, and a is a constant. From the equation, it can be seen that when the spacing of the precipitates decreases, the yield strength increases. Because of the larger volume fraction and the smaller dimension of precipitates, which leads to a finer spacing λ, alloy 2 has a higher strength than alloy 1.

The fracture surfaces shown in Figs.2 and 3 for alloy 1 and 2, respectively, suggest typical ductile fracture, which involves plastic deformation. As shown, second-phase particles (θ) are found at the dimple centers. Thus, these particles may be responsible for microcrack initiation due to the inherent incompatibility between the particles and the Al matrix during deformation. If this is so, the marked decrease in tensile elongation from alloy 1 to alloy 2 may be related to the corresponding increase in second-phase volume fraction with Ag addition. The reason is that when the second-phase spacing is reduced, there would be more extensive microcrack nucleation and, more importantly, microcrack linkup could be affected with great ease.

The effect of Ag addition on microstructure was discussed as follows. A previous study[18] indicated that in an Al-Cu-Mg alloy with Ag addition, Ag results in a dense distribution of small Cu atom clusters compared with that in a ternary alloy. To assume that the stimulated formation of Ω phase by Ag addition is attributed to the increased density of Mg/Cu/vacancy complexes because these complexes are an effective heterogeneous nucleation site for the Ω phase. At the early stage of nucleation of θ' and Ω particles, rapid clustering of Ag and Mg atoms occurs during artificial aging with no well-defined shape. Then Cu atoms assemble to these clusters, which initialize the growth of the clusters on the {111} planes with a platelet shape. These precipitates may be designated as the {111} GP zones in contrast to the normal Cu GP zones on {001} planes. They grow towards the lateral directions by subsequent aging and start to have structural features as the Ω phase. When the phase coarsens, the Mg and Ag atoms migrate from the interior of the precipitates to the surface. It is well known that the shape of the Cu GP zone is a thin plate on {001} planes. When {111} and {001} GP zones nucleate, they form at the same locations in the Al matrix, due to the decrease in nucleation energy of θ' and Ω platelets.

5 Conclusions

1) The Vickers hardness and strength of the Al-8Cu-0.5Mg alloy with Ag addition are much higher than its counterpart without Ag both at room- and elevated-temperatures.

2) The coexistence of θ' and Ω precipitates was found in the Ag-containing alloy, whereas only the θ' phase was observed in the Ag-free alloy. The dimension of the precipitates in the Ag-containing alloy is smaller and the volume fraction is higher than those in the Ag-free alloy. This may be the cause of the different properties observed for two alloys.

3) The small size and high volume fraction of θ' and Ω precipitates in the Ag-containing alloy improve the tensile strength and yield strength, especially in high temperatures. However, it is also responsible for the decrease in elongation, compared to the alloy without Ag, which is due to the microcrack because of inherent incompatibility between the particles and the Al matrix during deformation.

References

[1] RINGER S P, HONO K. Microstructural evolution and age hardening in aluminum alloys: Atom probe field-ion microscopy and transmission electron microscopy studies [J]. Mater Charact, 1999, 44(1): 101−131.

[2] FISHER J J. Aluminum alloy 2519 in military vehicles [J]. Advanced Materials and Processes, 2002, 160(9): 43−46.

[3] RINGER S P, SAKURAI T, POLMEAR I J. On the origins of hardening in Al-Cu-Mg-(Ag) alloys [J]. Acta Mater, 1997, 45(9):

3731−3744.

[4] MUKHOPADHYAY A K, RAMA RAO V V. Characterization of S (Al_2CuMg) phase particles present in as-cast and annealed Al-Cu-Mg(-Li)-Ag alloys [J]. Mater Sci Eng A, 1999, A268(1/2): 8−14.

[5] LI Shi-chen, ZHENG Zi-qiao. Computer simulation of distribution of the solutes in Al-Cu-(Mg)-(Ag) on initial aging stages [J]. J Cent South Univ Technol, 2000, 31(5): 441−444.

[6] CHESTER R J, POLMEAR I J. Precipitation in Al-Cu-Mg-Ag alloys [A]. In the Metallurgy of Light Alloys, Inst. of Metals [C]. London: Taylor & Francis Press, 1983. 75.

[7] KNOWLES K M, STOBBS W M. The structure of {111} age-hardening precipitates in Al-Cu-Mg-Ag alloys [J]. Acta Crystallography, 1988, B44(3): 207−227.

[8] MUDDLE B C, POLMEAR I J. The precipitate Ω phase in AL-Cu-Mg-Ag alloys [J]. Acta Metall Mater, 1989, 37(3): 777−789.

[9] CHANG Y C, HOWE J M. Composition and stability of Ω phase in an Al-Cu-Mg-Ag alloy [J]. Metall Trans A, 1993, A24(7): 1461−1470.

[10] GARG A, HOME J M. Convergent-beam electron diffraction analysis of the Ω phase in an Al-4.0Cu-0.5Mg-0.5Ag alloy [J]. Acta Metall Mater, 1991, 39(8): 1939−1946.

[11] RINGER S P, YEUNG W, MUDDLE B C, POLMEAR I J. Precipitate stability in Al-Cu-Mg-Ag alloys aged at high temperatures [J]. Acta Metall Mater, 1994, 42(5): 1715−1725.

[12] REICH L, MURAYAMA M, HONO K. Evolution of Ω phase in an Al-Cu-Mg-Ag alloy–A three dimensional atom probe study [J]. Acta Mater, 1998, 46(17): 6053−6062.

[13] XIAO D H, WANG J N, DING D Y, et al. Effect of Cu content on the mechanical properties of an Al-Cu-Mg-Ag alloy [J]. Journal of Alloys and Compounds, 2002, 343(1/2): 77−91.

[14] XIAO D H, WANG J N, DING D Y, CHEN S P. Effect of rare earth Ce addition on the microstructure and mechanical properties of an Al-Cu-Mg-Ag alloy [J]. Journal of Alloys and Compounds, 2003, 352(1/2): 84−88.

[15] YANG H L, WANG J N, XIAO D H, DING D Y. Study on solution heat treatment temperature of new Al-Cu-Mg-Ag alloy [J]. Ordnance Material Science and Engineering, 2003, 26(1): 16−18.

[16] XIAO D H, WANG J N, CHEN S P, DING D Y. Effect of Ce addition on microstructure and elevated temperature properties in Al-Cu-Mg alloy with high Cu/Mg ratio [J]. Journal of the Chinese Rare Earth Society. 2003, 21(5): 564−567.

[17] FENG D. Metals Physics[M]. Beijing: Science Press, 1999. 373.

[18] HIROSAWA S, SATO T, KAMIO A, FLOWER H M. Classification of the role of microalloying elements in phase decomposition of Al based alloys [J]. Acta Mater, 2000, 48(8): 1797−1806.

(Edited by LI Xiang-qun)